



ENGINEERING PHYSICS AND MATHEMATICS

A comparative study of leaves extracts for corrosion inhibition effect on aluminium alloy in alkaline medium



Namrata Chaubey^a, Dileep Kumar Yadav^b, Vinod Kumar Singh^a, M.A. Quraishi^{c,*}

^a Department of Chemistry, Udai Pratap Autonomous College, Varanasi 221002, India

^b Department of Ceramic Engineering, Indian Institute of Technology (Banaras Hindu University), Varanasi 221005, India

^c Department of Chemistry, Indian Institute of Technology (Banaras Hindu University), Varanasi 221005, India

Received 2 May 2015; revised 2 August 2015; accepted 31 August 2015

Available online 12 November 2015

KEYWORDS

Aluminium;
AFM;
EIS;
Polarization;
Alkaline corrosion

Abstract This paper deals with the comparative inhibition study of some plants leaves extract namely *Cannabis sativa* (CS), *Rauwolfia serpentina* (RS), *Cymbopogon citratus* (CC), *Annona squamosa* (AS) and *Adhatoda vasica* (AV) on the corrosion of aluminium alloy (AA) in 1 M NaOH. The corrosion tests were performance by using gravimetric, electrochemical impedance spectroscopy (EIS), potentiodynamic polarization and linear polarization resistance (LPR) techniques. RS showed maximum inhibition efficiency ($\eta\%$), 97% at 0.2 g L^{-1} . Potentiodynamic polarization curves justified that all the inhibitors are mixed-type. Surface morphology of AA is carried by scanning electron microscopy (SEM) and atomic force microscopy (AFM).

© 2015 Ain Shams University. Production and hosting by Elsevier B.V. This is an open access article under the CC BY-NC-ND license (<http://creativecommons.org/licenses/by-nc-nd/4.0/>).

1. Introduction

Aluminium and its alloys are finding wide applications in the various industries such as automotive, aerospace, construction and electrical power generation. Aluminium, with high energy density (8.1 kW h kg^{-1}) and an electrode potential of 2.35 V

vs. standard hydrogen electrode (SHE) in alkaline medium, has emerged as one of the most promising anode materials in Al–air cells [1]. These cells often utilize aluminium–alkaline solution systems. The corrosion (inherent dissolution) of aluminium in alkaline solution is detrimental to Al/air battery. It reduces the efficiency of battery and sometimes causes explosion as a result of hydrogen buildup [1,2].

The use of inhibitor is one of the most practical ways of reducing aluminium corrosion in alkaline medium. Few investigators have researched to lower the self-corrosion rate of aluminium through adding chemical compounds in alkaline solution [3–6]. However, most of them are hazardous, expensive and not safe for environment. In view of this, it is necessary to develop environmentally safe corrosion inhibitor for aluminium in alkaline medium; thus, we have chosen plant extracts as environmentally safe inhibitors that can be

* Corresponding author. Tel.: +91 9307025126; fax: +91 542 2368428.

E-mail addresses: maquraishi.apc@itbhu.ac.in, maquraishi@rediffmail.com (M.A. Quraishi).

Peer review under responsibility of Ain Shams University.



Production and hosting by Elsevier

extracted using simpler techniques with low cost. The phytochemicals (includes alkaloids, flavonoids) present in plant extract contain heteroatom such as N, S, O and π -electrons, aromatic ring, through which they adsorb on metal surface and inhibit corrosion.

There are only few reports available on the use of leaves extract as corrosion inhibitor for aluminium in alkaline medium in which authors obtained very good inhibition efficiency at very higher concentration [7–9]. Abiola et al. studied the effect of *Phyllanthus amarus* and *Gossypium hirsutum* leaves extract and found maximum inhibition efficiencies (76% and 97%) at 2.0 and 2.6 g L⁻¹ respectively on aluminium corrosion in alkaline medium [7,8]. Abdel-Gaber et al. showed maximum inhibition efficiency (88%) at optimum concentration (9.9 g L⁻¹) in the case of *Ambrosia maritime* leaf extract [9]. In the present study, a very small amount of concentration is sufficient to get better inhibition performance of investigated leaves. We have collected leaves of some medicinal plants; for instance, *Cannabis sativa* (f. Cannabaceae) is an annual, dioecious herb originating from Eastern and Central Asia. *Rauwolfia serpentina* (f. Apocynaceae), commonly known as Indian snake root, is widely grown in Southeastern Nigeria. *Cymbopogon citratus* (f. Poaceae), an herb known worldwide as lemongrass is tropical plant of Southeast Asia. *Annona squamosa* (f. Annonaceae), commonly famously known as Custard apple, is native to India. *Adhatoda vasica* (f. Acanthaceae), commonly known as Vasaka, is native to Asian countries.

The present investigation deals with the comparative inhibition effects of leaves extract namely *C. sativa* (CS), *R. serpentina* (RS), *C. citratus* (CC), *A. squamosa* (AS) and *A. vasica* (AV) on AA corrosion in 1 M NaOH. No report till date is available on the use of these leaves extracts as corrosion inhibitors for aluminium in alkaline medium. The inhibition performance is evaluated by electrochemical impedance spectroscopy (EIS), potentiodynamic polarization (PD) and linear polarization resistance (LPR) techniques and surface morphology was studied by SEM and AFM investigations.

2. Experimental procedure

2.1. Materials and test solution

The corrosion test was performed on the AA coupons with the composition given in Table 1. The test solution, 1 M NaOH was prepared by dissolving 40 g of NaOH in 1000 mL of double distilled water.

2.2. Preparation of leaves extracts

C. sativa (CS), *R. serpentina* (RS), *Cymbopogon citratus* (CC), *A. squamosa* (AS) and *A. vasica* (AV) plants were collected from the campus of Banaras Hindu University, India. Leaves were dried in oven at 45 °C, and grinded to powder. One gram of the powder was added to 500 mL of 1 M NaOH solution

and refluxed for 1 h. Thereafter, the mixture was cooled and filtered. The precipitate was dried and weighed. The extract was concentrated by evaporating the solvent and maintained its concentration to 1000 mg L⁻¹. Leaves extract test solutions were prepared at concentrations of 0.01, 0.05, 0.1 and 0.2 g L⁻¹.

2.3. Inhibitor constituents

The aqueous extract of leaves contains various chemical constituents such as the leaves of *A. vasica* (AV) contain alkaloids vasicine, N-oxides of vasicin, vasicinone, deoxyvasicine and maiontone [10]. Citral, geraniol and myricene are the water soluble active constituents present in the leaves of *C. citratus* (CC) [11]. Various indole alkaloids such as ajmalicine, ajmaline, reserpine and yohimbine are present in the leaf extract of *R. serpentina* (RS) [12]. The leaves of *C. sativa* (CS) contain various water soluble chemical constituents but cannabinoids (tetrahydrocannabinol, cannabidiol, cannabinol, tetrahydrocannabivarin and cannabigerol) are most interesting biologically active constituents [13]. The prevailing compounds of *A. squamosa* (AS) extract were sodium benzoate, butyloctylphthalate, 4-tert-butylcalix [4] arene and isoamylacetate [14]. The major active constituents present in inhibitor solutions are given in Table 2. These constituents contain π -bonds, nitrogen and oxygen atoms in their molecular structures as active centres. The various chemical constituents present in the inhibitor solutions were synergized the inhibition effect of each other.

2.4. Gravimetric and electrochemical experiments

The AA coupons used in gravimetric and electrochemical tests were mechanically cut into 2.5 × 2.0 × 0.046 cm and 7.0 × 1.0 × 0.046 cm dimensions, abraded with (600, 800, 1000 grade) silicon carbide papers, cleaned with acetone and dried at room temperature. Gravimetric experiment was conducted by placing the AA coupons into the test solutions for 3 h, and thereafter the samples were taken out, cleaned with distilled water, degreased with acetone, dried and weighed. The corrosion rate (C_R) was calculated by using following equation [15]:

$$C_R = \frac{87.6 \times w}{atd} \quad (1)$$

where t is the exposure time in hours (h), a is the area of a coupon in cm², w is the weight loss in grams (mg) and d is the density of AA in g cm⁻³.

With the calculated corrosion rate, the inhibition efficiency $\eta\%$ was calculated as follows:

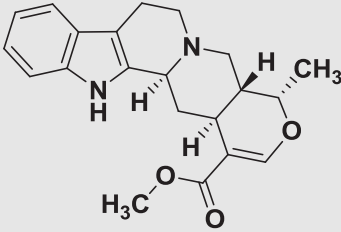
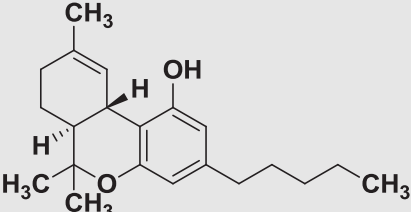
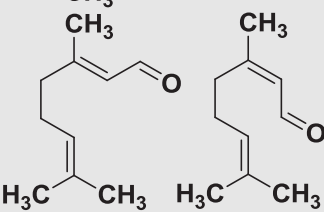
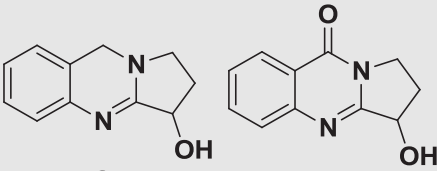
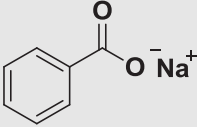
$$\eta\% = \frac{C_R - C_{R(i)}}{C_R} \times 100$$

and surface coverage (θ) values were calculated by the following equation:

Table 1 Chemical composition (wt%) of the AA used.

| Si | Fe | Cu | Mn | Mg | Zn | Cr | Ti | V | Ga | Al |
|------|------|------|------|------|------|------|------|------|------|----------|
| 0.77 | 0.93 | 0.02 | 0.11 | 0.01 | 0.01 | 0.05 | 0.02 | 0.01 | 0.01 | Balanced |

Table 2 Molecular structure of major constituents present in extracts.

| Inhibitors | Major constituents' | Molecular structure | Ref. |
|------------|---------------------------|---|------|
| RS | Ajmalicine |  | [11] |
| CS | Tetrahydrocannabinol |  | [12] |
| CC | Citral (Neral & Geranial) |  | [13] |
| AV | Vasicine and vasicinone |  | [14] |
| AS | Sodium benzoate |  | [15] |

$$\theta = \frac{C_R - C_{R(i)}}{C_R}$$

All the electrochemical tests were carried out in a conventional three-electrode cell consisting of an aluminium alloy (AA), a platinum foil and a saturated calomel electrode (SCE) as working, counter and reference electrodes respectively. The three electrode cell was connected to an electrochemical analyzer (Gamry Potentiostat/Galvanostat-Model 300). All tests were performed at 303 K. The working electrode was immersed in the test solution for 15 min before the measurements.

EIS measurements were carried out at OCP over a frequency range of 10^6 to 0.01 Hz using a 10 mV sine wave AC voltage. The linear polarization resistance study was carried out from the potential -0.02 V to $+0.02$ V vs. OCP at the scan rate of 0.125 mV/s. Potentiodynamic polarization measurements were carried out by sweeping the electrode potential from -0.25 V to $+0.25$ V vs. OCP at a scan rate of 1 mV/s. The data obtained from the electrochemical tests were analysed using Echem analyst 5.0 software.

2.5. Surface analysis

AA coupons of size $2 \times 2.5 \times 0.046$ were exposed in 1 M NaOH solution for 3 h in the absence and presence of optimum concentration of RS (showed maximum $\eta\%$). The SEM of the AA surface was performed at an accelerating voltage of 5000 V and $5000\times$ magnification using FEI Quanta 200F microscope. The AFM was performed using NT-MDT multimode, Russia, controlled by solver scanning probe microscope controller.

3. Results and discussion

3.1. Gravimetric measurements

3.1.1. Effect of inhibitor concentration

The corrosion rate (C_R) of AA coupons as a function of inhibitor concentration in 1 M NaOH solutions was determined at 303 K and summarized in Table 3. The corrosion rate decreased and inhibition efficiency ($\eta\%$) increased with

Table 3 Inhibition efficiency ($\eta\%$) and corrosion rate (C_R) values obtained from gravimetric test for AA in 1 M NaOH containing various concentrations of the inhibitors at 303 K.

| Inhibitors | C_{inh} (g L ⁻¹) | C_R (mm y ⁻¹) | θ (surface coverage) | η (%) |
|------------|-----------------------------------|--------------------------------|--------------------------------|---------------|
| Blank | 0.00 | 351 | – | – |
| RS | 0.01 | 99.6 | 0.711 | 71.1 |
| | 0.05 | 37.0 | 0.895 | 89.5 |
| | 0.10 | 17.7 | 0.952 | 95.2 |
| | 0.20 | 8.00 | 0.971 | 97.1 |
| | CS | 0.01 | 98.2 | 0.720 |
| CS | 0.05 | 41.8 | 0.882 | 88.2 |
| | 0.10 | 24.1 | 0.934 | 93.4 |
| | 0.20 | 11.2 | 0.967 | 96.7 |
| | CC | 0.01 | 129 | 0.630 |
| CC | 0.05 | 83.7 | 0.761 | 76.1 |
| | 0.10 | 59.5 | 0.834 | 83.4 |
| | 0.20 | 45.0 | 0.871 | 87.1 |
| | AV | 0.01 | 122 | 0.651 |
| AV | 0.05 | 66.0 | 0.816 | 81.6 |
| | 0.10 | 41.9 | 0.880 | 88.0 |
| | 0.20 | 41.8 | 0.910 | 91.2 |
| | AS | 0.01 | 145 | 0.570 |
| AS | 0.05 | 111 | 0.685 | 68.5 |
| | 0.10 | 69.2 | 0.802 | 80.2 |
| | 0.20 | 59.5 | 0.830 | 83.0 |

increase in inhibitor concentration. The lowest C_R and highest $\eta\%$ were obtained for RS at 0.2 g L⁻¹.

3.1.2. Effect of temperature

The $\eta\%$ decreased slightly with rise in temperature for inhibited systems for every 10 K rise in temperature from 303 to 333 K (Table 4) indicating better protection of AA at higher temperatures. The slight decrease of $\eta\%$ at higher temperatures might be due to weakening of adsorbed inhibitor film on the AA surface [16].

The apparent activation energy for corrosion reaction of AA in 1 M NaOH is calculated using Arrhenius equation:

$$\log C_R = \frac{-E_a}{2.303RT} + \lambda \quad (2)$$

E_a is the apparent activation energy for corrosion reaction, λ is Arrhenius pre-exponential factor and R is the gas constant. The E_a values were determined by linear regression between $\log C_R$ and $1/T$ (Fig. 1a). The E_a value in the absence of inhibitor is 33.6 kJ mol⁻¹ and in the presence of inhibitor i.e. RS, CS, AV, CC and AS is 80.7 kJ mol⁻¹, 69.2 kJ mol⁻¹, 53.9 kJ mol⁻¹, 52.7 kJ mol⁻¹ and 45.0 kJ mol⁻¹ respectively. Higher E_a values for inhibited systems suggest that the adsorbed inhibitor molecules on AA surface create a barrier for mass/charge transfer from the surface to the electrolyte [17].

3.1.3. Adsorption considerations

The surface coverage (θ) values corresponding to various concentrations of inhibitors have been used to explain the correct isotherm for adsorption process. Surface coverage (θ) values

Table 4 Parameters obtained from gravimetric test for AA in 1 M NaOH containing 0.2 g L⁻¹ concentrations of the inhibitors at different temperatures.

| Inhibitors | Temperature (K) | C_R (mm y ⁻¹) | η (%) |
|------------|-----------------|-----------------------------|------------|
| Blank | 303 | 351.0 | – |
| | 313 | 528.1 | – |
| | 323 | 885.6 | – |
| | 333 | 1127 | – |
| RS | 303 | 8.05 | 97.7 |
| | 313 | 22.5 | 95.7 |
| | 323 | 59.5 | 93.2 |
| | 333 | 111.3 | 90.1 |
| CS | 303 | 11.2 | 96.7 |
| | 313 | 32.2 | 93.9 |
| | 323 | 67.6 | 92.3 |
| | 333 | 136.8 | 87.8 |
| CC | 303 | 45.0 | 87.1 |
| | 313 | 86.95 | 83.5 |
| | 323 | 173.9 | 80.3 |
| | 333 | 239.8 | 78.2 |
| AV | 303 | 30.5 | 91.2 |
| | 313 | 64.4 | 87.8 |
| | 323 | 115.4 | 86.9 |
| | 333 | 214.1 | 81.0 |
| AS | 303 | 59.5 | 83.0 |
| | 313 | 99.4 | 81.1 |
| | 323 | 180.7 | 79.6 |
| | 333 | 257.3 | 77.1 |

were attempted to fit to different isotherms such as Freundlich, Temkin, Langmuir and Frumkin isotherms. The best fit was obtained with Langmuir isotherm which is represented by the following equation [18]:

$$\frac{C_{inh}}{\theta} = \frac{1}{K_{ads}} + C_{inh} \quad (3)$$

where K_{ads} is the adsorption equilibrium constant, and C_{inh} is the inhibitor concentration. Straight lines were obtained when we plot C_{inh}/θ against C_{inh} (Fig. 1b) which suggested the adsorption of inhibitors on the AA surface followed Langmuir adsorption isotherm. The adsorption equilibrium constant (K_{ads}) and free energy of adsorption (ΔG_{ads}°) were calculated using equation [19]:

$$K_{ads} = \frac{1}{C_{(sol.)}} \exp\left(\frac{\Delta G_{ads}^\circ}{RT}\right) \quad (4)$$

where R is universal gas constant, T is the absolute temperature and $C_{(sol.)}$ is the concentration of water (1000 g L⁻¹).

The values of K_{ads} and ΔG_{ads}° were calculated and are listed in Table 5. It is mentioned in various literature that the values of ΔG_{ads}° up to -20 kJ mol⁻¹ are consistent with electrostatic interaction between charged inhibitor molecules and a charged metal (physical adsorption), while those nearly -40 kJ mol⁻¹ or higher corresponds to the charge sharing or charge transfer from the inhibitor molecules to the metal surface to form a coordinate type bond (chemical adsorption) [20]. The calculated values of ΔG_{ads}° for studied inhibitors range from -25 to -30 kJ mol⁻¹. The values of K_{ads} decrease with increase in temperature. Higher values of K_{ads} mean better inhibition

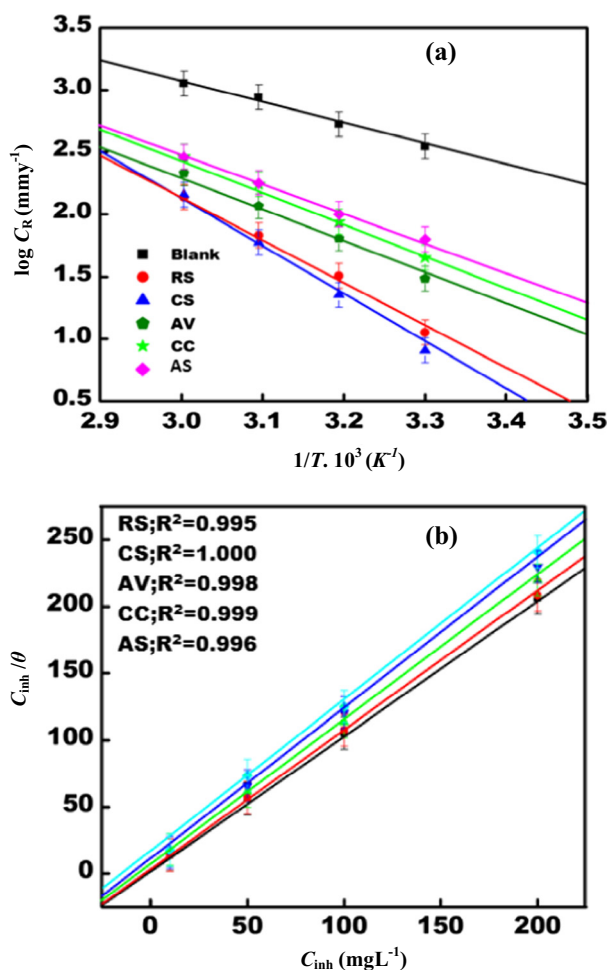


Figure 1 (a) Arrhenius plots for AA corrosion rates (C_R) in 1 M NaOH without and with optimum concentration (0.2 g L^{-1}) of inhibitors and (b) Langmuir adsorption isotherm plots for adsorption of inhibitors on AA in 1 M NaOH.

efficiency of an inhibitor and strong interaction between the inhibitor molecules and the metal surface [21].

3.2. Electrochemical investigations

3.2.1. Potentiodynamic polarization (Tafel) and linear polarization resistance

The Tafel curves of AA in 1 M NaOH solution in the absence and presence of optimum concentration of inhibitors at 303 K are shown in Fig. 2a. The linear section of cathodic and anodic Tafel lines was extrapolated to the corrosion potential in order to calculate associated polarization parameters such as corrosion potential (E_{corr}), corrosion current density (i_{corr}), anodic and cathodic Tafel slopes (β_a and β_c) which are tabulated in Table 6. The inhibition efficiencies using values of corrosion current density were calculated by the following equation [22]:

$$\eta\% = \frac{i_0 - i}{i_0} \times 100 \quad (5)$$

where i_0 and i are the corrosion current densities in the absence and presence of inhibitors, respectively. It is clear from Fig. 2a and Table 6 that all the inhibitors showed significant decrease

Table 5 Thermodynamic parameters for the adsorption of inhibitors on AA at 0.2 g L^{-1} in 1 M NaOH at different temperatures.

| Inhibitors | Temperature (K) | K_{ads} (g^{-1}) | G_{ads}° (kJ mol^{-1}) |
|------------|-----------------|--------------------------------------|---|
| RS | 303 | 161.6 | -30.21 |
| | 313 | 95.0 | -29.83 |
| | 323 | 66.4 | -29.82 |
| | 333 | 33.4 | -28.84 |
| CS | 303 | 120 | -29.46 |
| | 313 | 66.4 | -28.89 |
| | 323 | 50.5 | -29.08 |
| | 333 | 30.7 | -28.60 |
| CC | 303 | 33.4 | -26.24 |
| | 313 | 24.1 | -26.26 |
| | 323 | 20.0 | -26.59 |
| | 333 | 15.0 | -26.62 |
| AV | 303 | 50.5 | -27.28 |
| | 313 | 33.4 | -27.11 |
| | 323 | 25.0 | -27.19 |
| | 333 | 21.3 | -27.59 |
| AS | 303 | 23.05 | -25.31 |
| | 313 | 20.0 | -25.77 |
| | 323 | 14.23 | -25.68 |
| | 333 | 12.85 | -26.19 |

in corrosion current density (i_{corr}) and increase in inhibition efficiency ($\eta\%$) at their optimum concentrations. The lowest value of i_{corr} was obtained for RS at its optimum concentration which is reflected in its highest inhibition efficiency. According to the literature, if the shift in E_{corr} value for inhibited system is more than $\pm 85 \text{ mV}$ with respect to uninhibited system then the inhibitor can be regarded as anodic or cathodic type [23]. Any noticeable shifts were not observed in E_{corr} values for RS, AS and CS with respect to the uninhibited system (Fig. 2a and Table 6) indicating mixed mode of corrosion inhibition. However, the E_{corr} values of AV and CC were slightly shifted in the cathodic direction (up to 30 mV) suggesting mixed-mode of corrosion inhibition with slight cathodic effect.

Table 6 also provides the polarization resistance (R_p) values at optimum concentration of all the inhibitors. R_p values were calculated from the slope of electrode potential and current density relationship. The inhibition efficiency was calculated using R_p values by the following equation [24]:

$$\eta\% = \left(1 - \frac{R_p}{R_{p(i)}}\right) \times 100 \quad (6)$$

where R_p and $R_{p(i)}$ are the polarization resistances in the absence and presence of inhibitors, respectively. It was noticed that polarization resistance values were higher for inhibited systems than uninhibited system. The higher R_p values in inhibited systems suggested the inhibition of AA corrosion in alkaline medium [24].

3.2.2. Electrochemical impedance spectroscopy

The corrosion behaviour of AA was also investigated using electrochemical impedance technique at the optimum concentration of inhibitors in 1 M NaOH at 303 K. Nyquist plots (Fig. 2b) depict the similar shape in the absence and presence

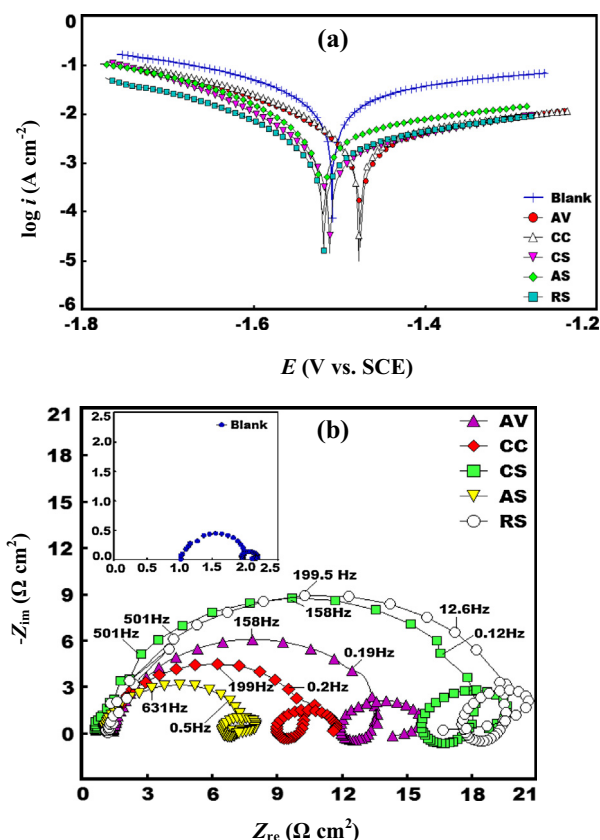


Figure 2 (a) Potentiodynamic polarization curves of AA in 1 M NaOH without and with optimum concentration (0.2 g L^{-1}) of inhibitors at 303 K and (b) Nyquist plots of AA in 1 M NaOH without and with optimum concentration (0.2 g L^{-1}) of inhibitors at 303 K.

of inhibitors indicating that there is no change in corrosion mechanism occurring through the inhibitors. The impedance plots feature a capacitive time constant in high frequency zone and another capacitive time constant in low frequency zone separated by an inductive time constant in medium frequency zone. After addition of inhibitors, the diameter of the capacitive loops increased and was a maximum in the case of RS. The capacitive loop in high frequency zone is ascribed to charge transfer of the corrosion process and to the pre-formed oxide layer. The oxide layer is considered to be a parallel circuit of a resistor due to ionic conduction in the oxide film and a capacitor due to its dielectric properties [25]. According to Brett, the first capacitive time constant corresponds to interfa-

cial reactions of Al oxidation at the metal/oxide/electrolyte interface. In this process, the formation of Al^+ ions at the metal/oxide interface and their migration through oxide layer to the oxide/solution interface occur due to high electric field strength, where they get oxidized to Al^{3+} [26,27]. The inductive loop in intermediate frequency zone is attributed to relaxation of the adsorbed intermediates (OH_{ads}) to the oxide layer of metal surface. The second capacitive loop in the low frequency region could be assigned to the dissolution of the AA in alkaline medium [25].

Fig. 3a and b shows the simulated and experimentally generated Bode phase angle plots and Nyquist plots. The EIS parameters were obtained by fitting an equivalent circuit model displayed in Fig. 3c. This model consists of a solution resistance (R_s), inductance (L), resistance associated with inductance (R_L), charge transfer resistances (R_{ct}) and constant phase element (CPE). It is noticeable that surface imperfections have profound effect on double layer capacitance (C_{dl}) which is simulated via CPE. The CPE used in equivalent circuit is defined by the components Q and n and is deduced by the following relation [28]:

$$Z_{\text{CPE}} = \left(\frac{1}{Q(j\omega)^n} \right) \quad (7)$$

where Q is the proportionality constant and comparable to capacitance, j is the imaginary unit and ω is the angular frequency ($\omega = 2\pi f_{\text{max}}$, f_{max} is the frequency at maximum in Hz), and n is phase shift and related to degree of surface non-homogeneity. The CPE is described by the value of n . The CPE represents resistance if ($n = 0$, $Q = R$), capacitance ($n = 1$, $Q = C$), inductance ($n = -1$, $Q = L$) and Warburg impedance ($n = 0.5$, $Q = W$). In the present study, the value of n varies from 0.898 to 0.999 in the presence of inhibitors indicating the resemblance of CPE with capacitor [29]. The double layer capacitance (C_{dl}) is deduced from the following equation:

$$C_{\text{dl}} = Q \times (2\pi f_{\text{max}})^{n-1} \quad (8)$$

Inspection of Table 7 reveals that the C_{dl} values reduce while R_{ct} values enhance in inhibited systems than in uninhibited system. Decrease of C_{dl} in inhibited systems can result from the decrease in local dielectric constant (removal of high dielectric water with lower dielectric inhibitor molecules) suggesting the inhibitor molecules function by adsorption at the metal/electrolyte interface [30]. The R_{ct} is inversely proportional to the corrosion rate; hence the higher R_{ct} values show the slower corroding system. The maximum R_{ct} value ($18.26 \text{ } \Omega \text{ cm}^2$) and lowest C_{dl} value ($48.59 \text{ } \mu\text{F cm}^{-2}$) were obtained for RS at its optimum concentration.

Table 6 Electrochemical polarization parameters for AA in 1 M NaOH in the absence and presence of 0.2 g L^{-1} concentrations of the inhibitors at 303 K.

| Inhibitors | Tafel polarization | | | | | Linear polarization | | | |
|------------|---|---------------------------|-------------------|-------------------|------------|------------------------------------|------------------------------|----------|------------|
| | i_{corr} (mA cm^{-2}) | E_{corr} (V/SCE) | β_a (V/dec) | β_c (V/dec) | η (%) | R_p ($\Omega \text{ cm}^{-2}$) | C_R (mm y^{-1}) | θ | η (%) |
| Blank | 96.3 | -1.508 | 1.001 | 0.504 | - | 1.279 | 347.0 | - | - |
| RS | 2.43 | -1.519 | 0.628 | 0.173 | 97.4 | 20.20 | 6.221 | 0.94 | 94.0 |
| CS | 4.21 | -1.512 | 0.517 | 0.127 | 95.6 | 18.25 | 7.126 | 0.93 | 93.1 |
| CC | 9.92 | -1.478 | 1.523 | 0.167 | 89.6 | 9.698 | 39.41 | 0.86 | 86.8 |
| AV | 6.51 | -1.476 | 0.747 | 0.164 | 93.2 | 15.81 | 30.13 | 0.91 | 91.9 |
| AS | 14.71 | -1.519 | 1.755 | 0.174 | 84.7 | 7.254 | 56.89 | 0.82 | 82.4 |

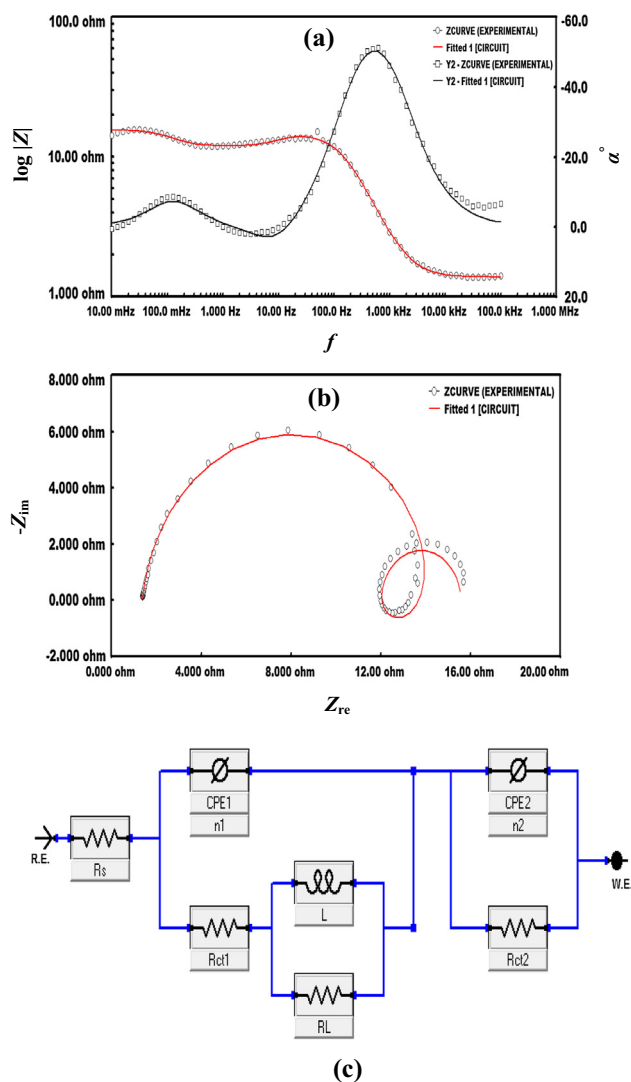


Figure 3 Simulated and experimentally generated EIS plots (a) Bode phase angle, (b) Nyquist plot and (c) electrical equivalent circuit used for the analysis of impedance spectra.

Fig. 4a and b shows the Bode magnitude and bode phase angle plots in the absence and presence of optimum concentration of inhibitors. The slope value of Bode plot (S) and phase angle (α°) are important factors to define a domain of pure capacitive behaviour. For an ideal capacitor, the value of S

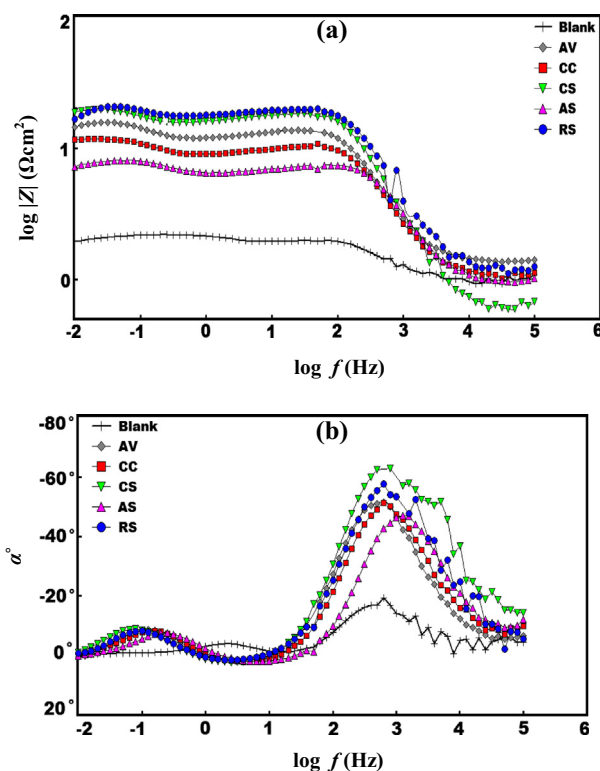


Figure 4 Impedance spectra of AA in 1 M NaOH without and with optimum concentration (0.2 g L^{-1}) of inhibitors at 303 K (a) Bode magnitude ($\log f$ vs. $\log |Z|$) and (b) Bode phase angle plots ($\log f$ vs. α°).

and α° should be -1° and -90° , respectively. In present investigation, the maximum slope value reaches up to -0.75 and maximum phase angle was -58° suggesting deviation from pure capacitive behaviour [31].

3.3. Surface investigations

3.3.1. Scanning electron microscopy

Fig. 5a shows the SEM micrograph of the uninhibited AA surface. The resulting micrograph reveals the greatly damaged surface with clearly visible cracks and pits. Fig. 5b displays the AA surface after the corrosion test in the presence of optimum concentration (0.2 g L^{-1}) of RS. It presents a smooth and clean surface in comparison with uninhibited AA surface,

Table 7 Electrochemical impedance parameters for AA in 1 M NaOH in the absence and presence of 0.2 g L^{-1} concentrations of the inhibitors at 303 K.

| Inhibitors | R_s (Ω) | Q_1 ($\text{S } \Omega^{-1} \text{ cm}^{-2}$) | n_1 | $(R_{ct})_1$ ($\Omega \text{ cm}^2$) | L (H cm^2) | R_L ($\Omega \text{ cm}^2$) | Q_2 ($\text{S } \Omega^{-1} \text{ cm}^{-2}$) | n_2 | $(R_{ct})_2$ ($\Omega \text{ cm}^2$) | C_{dl} ($\mu\text{F cm}^{-2}$) | η (%) |
|------------|-----------------------|--|-------|---|----------------------------|------------------------------------|--|-------|---|---------------------------------------|---------------|
| Blank | 1.023 | 500×10^{-6} | 0.975 | 0.849 | 0.221 | 0.121 | 39.8×10^{-6} | 0.521 | 0.188 | 413.8 | – |
| RS | 1.150 | 99.3×10^{-6} | 0.998 | 19.05 | 0.024 | 3.747 | 9.1×10^{-3} | 0.580 | 1.141 | 48.59 | 95.5 |
| CS | 1.576 | 116×10^{-6} | 0.904 | 16.68 | 0.042 | 4.059 | 11.2×10^{-3} | 0.530 | 1.531 | 60.44 | 94.8 |
| CC | 1.060 | 195×10^{-6} | 0.899 | 8.638 | 0.013 | 2.265 | 1.6×10^{-3} | 0.524 | 2.511 | 113.2 | 90.1 |
| AV | 1.927 | 114×10^{-6} | 0.999 | 13.88 | 0.042 | 0.005 | 99×10^{-3} | 0.555 | 3.412 | 96.09 | 93.7 |
| AS | 1.946 | 329×10^{-6} | 0.898 | 6.314 | 0.004 | 1.465 | 100×10^{-3} | 0.539 | 1.599 | 151.2 | 86.5 |

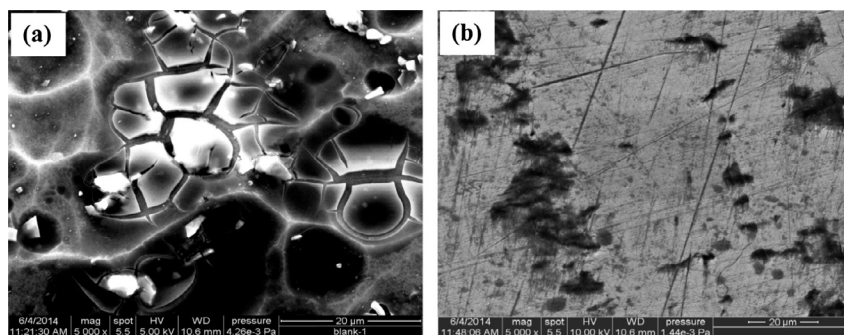


Figure 5 SEM micrographs of (a) uninhibited and (b) inhibited AA sample containing 0.2 g L^{-1} of RS in 1 M NaOH.

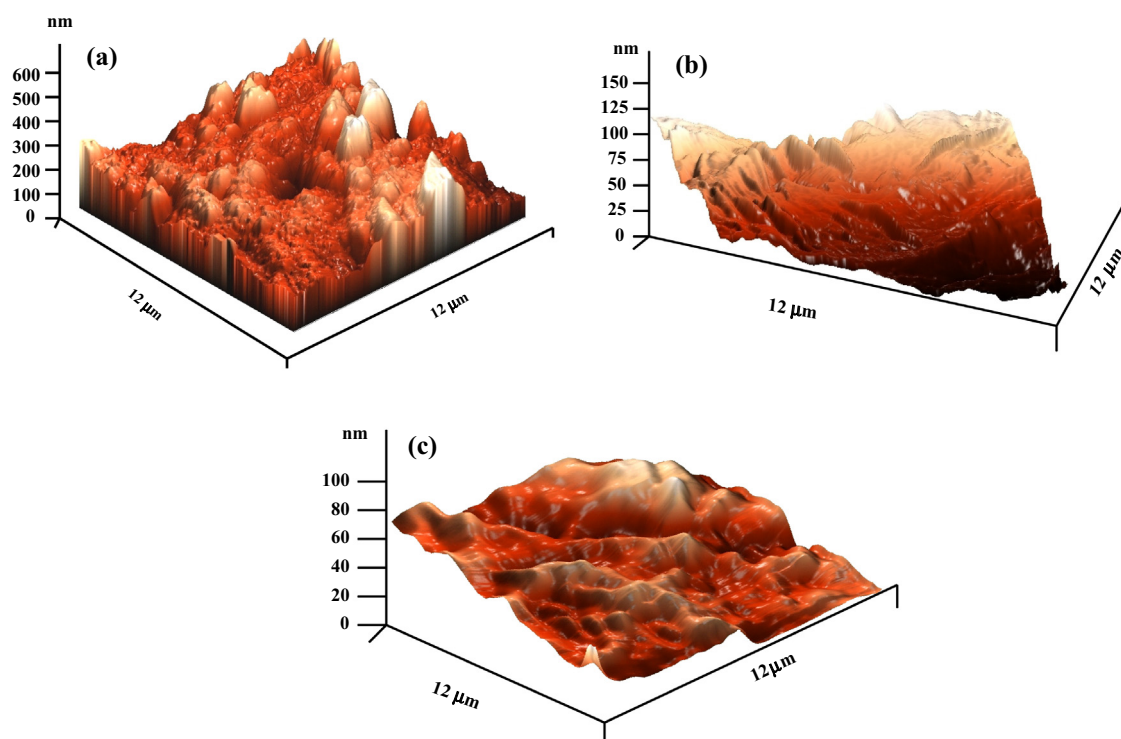


Figure 6 AFM three dimensional images of (a) uninhibited, (b) grounded and (c) inhibited AA sample containing 0.2 g L^{-1} of RS in 1 M NaOH.

which indicates that the adsorbed inhibitor molecules present in the extract of RS inhibit the corrosion of AA in alkaline medium.

3.3.2. Atomic force microscopy

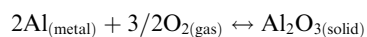
Further investigation of the corrosion inhibition ability of the extract was carried out by means of atomic force microscopy (AFM) in order to characterize the AA surface microstructure. Fig. 6 depicts three-dimensional AFM images of AA surface after 3 h exposure in 1 M NaOH at 303 K. In uninhibited system, the AA surface was fairly damaged due to dissolution in corrosive medium (Fig. 6a) with maximum height scale of 600 nm. The maximum height scale of grounded AA surface before exposure to corrosive solution was 150 nm (Fig. 6b). The maximum height scale of inhibited AA surface (Fig. 6c) was 100 nm due to formation of a protective layer on surface

which causes the decrease of AA surface roughness and effectively protects AA from corrosion.

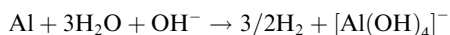
3.4. Explanation for inhibition

The extract of leaves in our study contains various naturally occurring chemical compounds. The principal chemical constituent of the aqueous extract of leaves is given in Table 2.

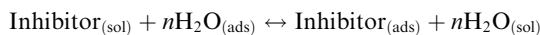
It is generally assumed that aluminium has great affinity for ambient oxygen for the formation of protective oxide layer:



The oxide film formed acts as a static barrier that isolates the metal from the solution. However, alkaline solutions may affect its properties. In alkaline solution the direct dissolution of aluminium is due to the following reaction [32]:



The soluble complex ion formed leads to the dissolution of the metal. The adsorption of inhibitor molecules is often a displacement reaction involving removal of adsorbed water molecules from the metal surface [33].



The inhibition is chiefly attributed to the presence of various organic compounds in the extract of plant leaves. The inhibitors may get adsorbed on the surface of aluminium and a protective film is formed. This restricts the diffusion of ions to or from the metal surface and hence retards the overall corrosion process. The interactions of the adsorbed inhibitor molecules with the metal surface may prevent the metal atoms from participating in the anodic reaction of the corrosion. This simple blocking effect decreases the number of metal atoms participating and hence decreases the corrosion rate [33].

4. Conclusions

Based on results of experimental investigation following conclusions are drawn:

1. The extract of plant leaves such as RS, CS, CC, AV and AS is good, environmentally benign inhibitors for corrosion control of AA in 1 M NaOH solution.
2. Inhibition efficiency increases with increase in concentration of extracts. RS showed maximum efficiency (97.1%) at its optimum concentration (0.2 g L⁻¹).
3. Inhibition efficiency decreases slightly with increase in temperature from 303 to 333 K.
4. The adsorption of inhibitors on the AA surface follows Langmuir adsorption isotherm.
5. All the inhibitors acted as mixed-type by inhibiting anodic and cathodic reactions to the nearly same extent.
6. The inhibition efficiencies obtained from gravimetric, potentiodynamic polarization and electrochemical impedance measurements are in good agreement.

Acknowledgement

I gratefully acknowledge Prof. M. A. Quraishi, Department of Chemistry, Indian Institute of Technology (Banaras Hindu University), Varanasi, INDIA, for facilitation of my research work.

References

- [1] Wang L, Wang W, Yang G, Liu D, Xuan J, Wang H, Leung MKH, Liu F. *Int J Hydrogen Energy* 2013;38:14801–9.
- [2] Oguzie EE. *Corros Sci* 2007;49:1527–39.
- [3] Maayta AK, Al-Rawashdeh NAF. *Corros Sci* 2004;46:1129–40.
- [4] Lashgari M, Malek AM. *Electrochim Acta* 2010;55:5253–7.
- [5] Soliman HN. *Corros Sci* 2011;53:2994–3006.
- [6] Rajendran S, Thangavelu C, Annamalai G. *J Chem Pharm Res* 2012;11:4836–44.
- [7] Abiola OK, Otaigbe JOE. *Corros Sci* 2009;51:2790–3.
- [8] Abiola OK, Otaigbe JOE, Kio OJ. *Corros Sci* 2009;51:1879–81.
- [9] Abdel-Gaber AM, Khamis E, Abo-EIDahab H, Adeel S. *Mater Chem Phys* 2008;109:297–305.
- [10] Singh MR. *J Mater Environ Sci* 2013;4:117–26.
- [11] Barbosa LCA, Pereira UA, Martinazzo AP, Maltha CRA, Teixeira RR, Melo EC. *Molecules* 2008;13:1864–74.
- [12] Deshmukh SR, Ashrit DS, Patil BA. *Int J Pharm Pharm Sci* 2012;4:329–34.
- [13] Audu BS, Ofojekwu PC, Ujah A, Ajima MNO. *J Phytol* 2014;3:35–43.
- [14] Vanitha V, Umadevi KJ, Vijayalakshmi K. *Int J Pharm Sci Drug Res* 2011;3:309–12.
- [15] ASTM G1. Standard practice for preparing, cleaning, and evaluating corrosion test specimens; 2003.
- [16] Li X, Deng S, Xie X. *J Taiwan Inst Chem E* 2014;45:1865–75.
- [17] Yadav DK, Quraishi MA, Maiti B. *Corros Sci* 2012;55:254–66.
- [18] Ramya K, Mohan R, Anupama KK, Joseph A. *Mater Chem Phys* 2015;149–150:632–47.
- [19] Yadav DK, Quraishi MA. *Ind Eng Chem Res* 2012;51:14966–79.
- [20] Zhang Y, Nie M, Wang X, Zhu Y, Shi F, Yu J, Hou B. *J Hazard Mater* 2015;289:130–9.
- [21] Abd El Rehim SS, Sayyah SM, El-Deeb MM, Kamal SM, Azooz RE. *Mater Chem Phys* 2010;123:20–7.
- [22] Zhao J, Duan H, Jiang R. *Corros Sci* 2015;91:108–19.
- [23] Yadav DK, Chauhan DS, Ahamad I, Quraishi MA. *RSC Adv* 2013;3:632–46.
- [24] Solmaz R. *Corros Sci* 2014;79:169–76.
- [25] Kumari PDR, Nayak J, Shetty AN. <http://dx.doi.org/10.1016/j.arabjc.2011.12.003>.
- [26] Brett CMA. *Corros Sci* 1992;33:203–10.
- [27] Prabhu D, Rao P. <http://dx.doi.org/10.1016/j.arabjc.2013.07.059>.
- [28] Naderi E, Jafari AH, Ehteshamzadeh M, Hosseini MG. *Mater Chem Phys* 2009;115:852–8.
- [29] Khaled KF. *J Appl Electrochem* 2011;41:277–87.
- [30] Yadav DK, Quraishi MA. *Ind Eng Chem Res* 2012;51:8194–210.
- [31] Hassan HH, Amin MA, Gubbala S, Sunkara MK. *Electrochim Acta* 2007;52:6929–37.
- [32] Zhang J, Klasky M, Letellier BC. *J Nucl Mater* 2009;384:175–89.
- [33] Prabhu D, Rao P. *J Environ Chem Eng* 2013;1:676–83.



Namrata Chaubey is a research scholar, doing Ph.D from Udai Pratap College, Varanasi under the supervision and co supervision of Dr. Vinod Kumar Singh and Prof. M. A. Quraishi respectively.



Dileep Kumar Yadav has completed his Ph.D in the field of corrosion from Department of chemistry and his post doc as a Research Associate from Department of Ceramic Engineering, IIT, BHU. He is having more than 10 publications. Currently, he is working as a Quality control officer in Indian Oil Corporation Ltd. (Assam).



Vinod Kumar Singh is an associate professor in Udai Pratap College, Varanasi. He has been completed his Ph.D from department of chemistry, BHU. His area of interest is corrosion and green chemistry.



M.A. Quraishi is a professor in the Department of Chemistry Indian Institute of Technology, BHU, Varanasi. His area of interest is corrosion and green Chemistry. He is fellow of Royal Society.